Synthesis and Characterization of Phthalocyanines with Direct Si–Si Linkages

Nagao Kobayashi,*[a] Fumio Furuya,[a] Gyeong-Chang Yug,[b] Hisanobu Wakita,[c] Mitsutoshi Yokomizo,[c] and Naoto Ishikawa[d]

Abstract: Several cofacial phthalocyanines (Pcs) with an Si–Si linkage were obtained by one-step condensation of 1*H*-isoindole-1,3(2*H*)-diimine with hexachlorodisilane as template in quinoline. They were characterized by gel-permeation chromatography, IR, NMR spectroscopy, and mass spectrometry, and cyclic voltammetry. The results strongly suggest that we indeed obtained Pc dimers directly linked by an Si–Si bond using this novel concept of utilizing a compound/salt with an element–element bond as a template. The cofacial dimer structures are reasonably supported by X-ray absorption near-edge structure (XANES), electronic absorption and magnetic circular dichroism (MCD) spectra, and molecular orbital (MO) calculations. Interestingly, they show an electronic absorption spectrum very similar to that of silicon tetrabenztriazacorrole (SiTBC).

Keywords: electronic structure · phthalocyanines · silicon · structure elucidation · tetrabenztriazacorrole

Introduction

It is possible that two structurally different compounds may show very similar electronic absorption spectra, although this is not common. For example, the spectra of phthalocyaninatonickel(II) and bis(β-diiminotetracyanopyrrolizinato)nickel(II) resemble each other in both the visible and ultraviolet regions, although their ligands have quite different structures.[1] However, this is an unusual example, and in most cases different compounds (structures) give different spectra. A few years ago, we reported[2] the synthesis and electronic absorption spectrum of an SiPc dimer with a direct Si–Si link, which was obtained by a one-pot template reaction. At that time, the Si–Si Pc dimer was not extensively characterized. Subsequently, we noticed that its electronic absorption spectrum is very similar to that previously reported for SiTBC by Fujiki et al. (Figure 1),[3] and this unexpected similarity was also pointed out by others in personal communications. It therefore became neccesary to prove whether or not our SiPc really is the desired Si–Si linked Pc dimer, and accordingly we have carried out further experiments and reexamined our results and literature data on SiTBC.[3, 4] To reduce the possibility of erroneous conclusions, we synthesized several other Si–Si Pcs by the same method,[2] and characterized them by as thoroughly as possible. As will be shown here, the results of gel-permeation chromatography (GPC), NMR and IR spectroscopy, mass spectrometry, and cyclic voltammetry (CV) clearly indicate that our Pcs indeed have a size typical

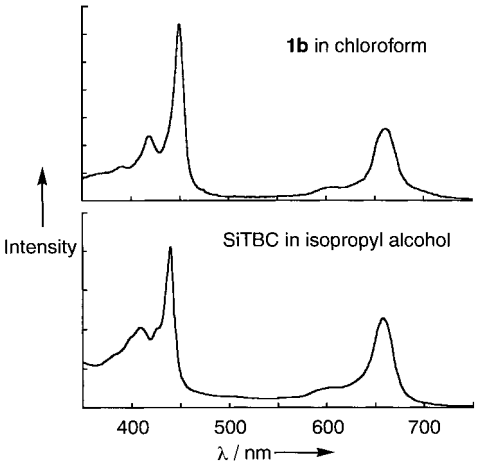

Figure 1. Absorption spectra of **1b** in chloroform and that reported by Fujiki et al. for SiTBC in isopropyl alcohol (redrawn from ref. [3]).

[a] Prof. Dr. Dr. N. Kobayashi, F. Furuya
Department of Chemistry, Graduate School of Science
Tohoku University, Sendai 980-8578 (Japan)
Fax: (+81) 22-217-7719
E-mail: nagaok@mail.cc.tohoku.ac.jp

[b] Dr. G.-C. Yug
Institute for Chemical Reaction Science
Tohoku University, Sendai 980-8577 (Japan)

[c] Prof. Dr. H. Wakita, Dr. M. Yokomizo
Department of Chemistry, Faculty of Science
Fukuoka University
8-19-1 Nanakuma, Jonan-ku, Fukuoka 814-0180 (Japan)

[d] Prof. Dr. N. Ishikawa
Department of Chemistry, Tokyo Institute of Technology
O-okayama, Meguro-ku, 152-8551 (Japan)

Supporting information for this article is available on the WWW under http://www.wiley-vch.de/home/chemistry/ or from the author.

0947-6539/02/0806-1474 $ 17.50+.50/0

of Pc dimers, and therefore that we have obtained the desired Si–Si Pc dimers. To strengthen our conclusion, the compounds were further characterized by NMR spectroscopy, X-ray absorption near-edge structure (XANES), and magnetic circular dichroism (MCD). In addition, molecular orbital (MO) calculations also succeeded in reasonably explaining the cofacial dimer structure in these compounds. We finally succeeded in obtaining single crystals of SiTBC suitable for X-ray analysis. This SiTBC is, of course, different from the above Si–Si Pc dimers in its size and electrochemical behavior, but displays an electronic absorption spectrum similar to those of Si–Si Pc dimers. The spectrum of SiTBC was also approximately reproduced by MO calculations.

Results and Discussion

Synthesis, purification, and stability

General: Si–Si Pc dimers with two axial Cl ligands such as **1a** and **3a** were synthesized at 180–190 °C under a nitrogen atmosphere.[5] At reflux, however, the Si–Si bond was cleaved, and only monomers such as **2a**, **2b**, **4a**, and **4b** (Figure 2) were obtained. The reaction was carried out under a nitrogen atmosphere, since O_2 or H_2O can convert the Si–Si bond into Si-O-Si, particularly at higher temperatures.[6] The highest yields of Si–Si dimers **1a** and **1b** were 31–36%, which is remarkably high, since the yields of the corresponding monomer from $SiCl_4$ and 1*H*-isoindole-1,3(2*H*)-diimine derivatives are generally at most 30–50%.[7] After the reaction, GPC was used to separate the desired dimers from the accompanying monomers. The first band was always that of the desired dimer (see below).

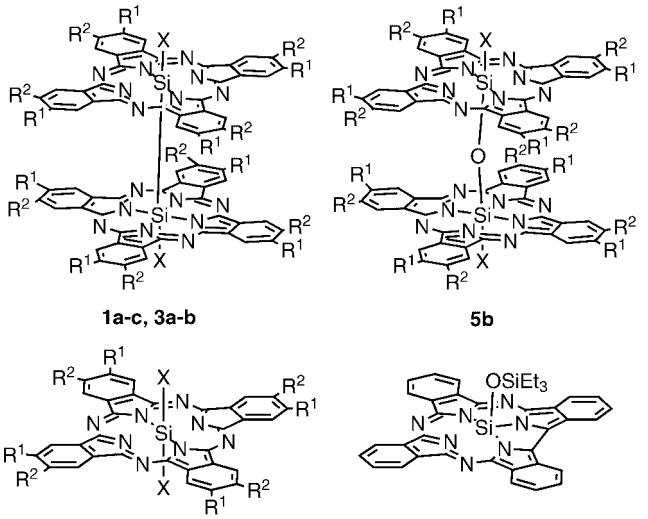

Compound		R^1	R^2	X
Si-Si dimer	**1a**	*n*BuO-	*n*BuO-	-Cl
	1b	*n*BuO-	*n*BuO-	-OH
	1c	H	H	-OH
	3a	*t*Bu-	H	-Cl
	3b	*t*Bu-	H	-OH
Si monomer	**2a**	*n*BuO-	*n*BuO-	-Cl
	2b	*n*BuO-	*n*BuO-	-OH
	2c	*n*BuO-	*n*BuO-	-OMe
	4a	*t*Bu-	H	-Cl
	4b	*t*Bu-	H	-OH
μ-oxo dimer	**5b**	*t*Bu-	H	-OH

Bu- = C_4H_9-

Figure 2. Structures of the SiPc monomers and dimers and an SiTBC.

NMR spectra: The ^{1}H NMR spectra of *tert*-butylated Pcs have a complex splitting pattern in the aromatic region because of the presence of various isomers, even in the monomeric state. Peripherally octaalkoxylated Pcs generally show simpler patterns because they are single isomers. Dimeric octabutoxy Pc **1b** showed a broad peak corresponding to 16 aromatic protons at $\delta = 8.5$. Although two small peaks were often superimposed on this broad peak when the spectrum was recorded in $CDCl_3$, it became a single peak in benzene (Figure 3). The OCH_2 protons of the butoxy group appeared in the region around $\delta = 3.5-4$, and the other alkyl protons at

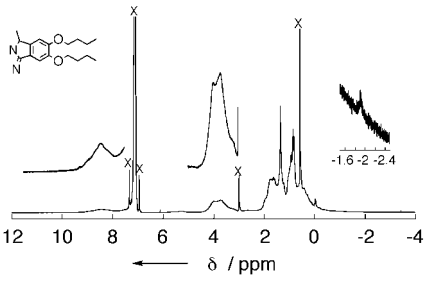

Figure 3. ^{1}H NMR spectrum of Si–Si Pc dimer **1b** in C_6D_6. Signals of the solvent and side bands are marked with an x.

Abstract in Japanese:

金属フタロシアニン(MtPc)は、しばしば金属塩/化合物を鋳型として合成される。鋳型となる化合物中に金属—金属直接結合があれば、その両方の金属を鋳型として一度に対面型で且つ金属—金属直接結合を有する MtPc ダイマーを合成できる可能性がある。そこで Cl_3Si-$SiCl_3$ を鋳型として Si-Si 直接結合の Pc ダイマーを、一段階で約 30%の収率で合成し、NMR、Mass、XANES、電子吸収、磁気円偏光二色性の各種分光法、それにサイズ排除カラムクロマトグラフィー、電気化学的測定で特性化し、更に分子軌道計算により、性質の幾つかの解釈を試みた。この化合物の電子吸収スペクトルでは、通常の Pc には見られない約 445 nm に非常に強い吸収帯が現れ、計算からは、Si-Si 間のσ結合から配位子への電荷移動帯と帰属された。また今回の Pc は対面型2量体であるにもかかわらず、電子吸収スペクトルが、テトラベンズトリアザコロール単量体のそれと非常に似ているという特徴を有する。

  0947-6539/02/0806-1475 $ 17.50+.50/0

$\delta = 0-2$, while the two SiOH protons were observed at $\delta = -1.91$ due to the ring current of the Pc. The overall spectroscopic pattern is similar to that observed for cation-containing cofacial crown-Pc dimers.[8]

X-ray crystallography: The most effective way to prove a structure is to obtain X-ray crystallographic data. One referee thought that our dimers might be SiTBC or derivatives thereof (e.g., dimers). To eliminate this ambiguity, we unsuccessfully attempted to obtain single crystals of Si–Si Pc dimers with a diversity of substituents (methoxy, ethyl, ethoxy, and butoxy) under various conditions over a period of six months. In the course of time, the color of the Pc solutions changed, which suggested decomposition of compounds. The Si–Si Pc dimers are relatively stable when stored in the dark as a powder, but gradually decompose in solution. However, the SiTBC monomer **6** was obtained as a by-product of the synthesis of **1b**, and crystals suitable for X-ray analysis were grown from benzene. Figure 4 shows the ORTEP plot of **6**,[9] which has a tetrabenztriazacorrole structure with a single

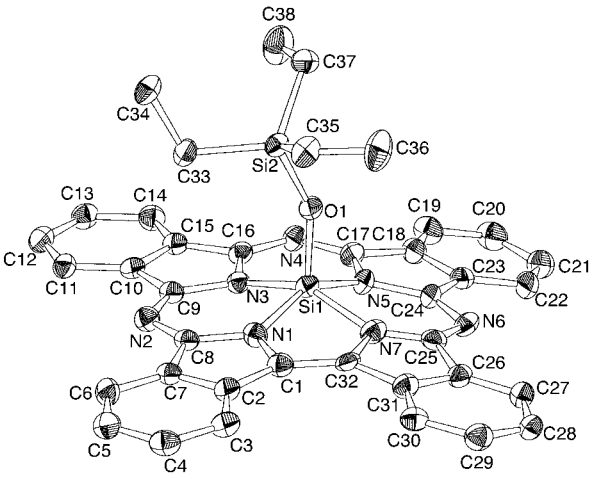

Figure 4. Structure of **6** (ORTEP plot; thermal ellipsoids are drawn at the 30% probability level. One molecule excluding disordered atoms is shown. Hydrogen atoms are omitted for clarity.

axial triethylsiloxy ligand and four equivalent pyrrole nitrogen atoms. One isoindole ring (N7-C25–C32) of **6** is disordered. The TBC plane is domed, and the distance between Si1 and the N4 mean plane (N1-N3-N5-N7) is 0.44 Å. This compound was later used as a standard in gel-permeation chromatography and electrochemistry to prove that our Si–Si Pc dimers are different from SiTBC and much larger in size.

Identification of the dimeric structure

Gel-permeation chromatography:[10] Estimation of the size of the target compound is important, particularly since an Si–Si bond is weaker than a C–C bond.[6] Figure 5 shows the GPC separation characteristics on Bio-beads S-X1 (Bio-rad) with chloroform for three *tert*-butylated SiPcs with two axial OH ligands and SiTBC **6**. Table 1 compares the elution velocities. As can be seen, the velocity of the Si–Si dimer **3b** (0.50 cm min^{-1}) is very close to that of the μ-oxo dimer **5b**

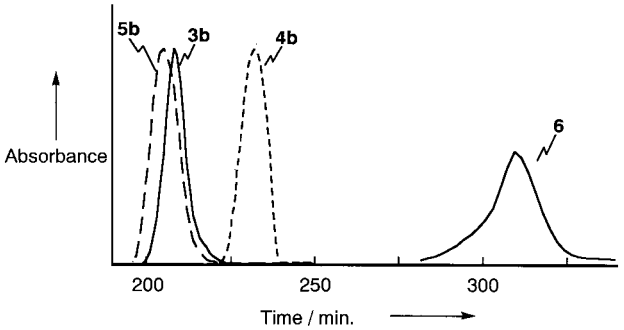

Figure 5. Gel-permeation chromatograms, obtained separately but superimposed, for **3b** (Si–Si dimer), **4b** (monomer), **5b** (μ-oxo dimer) and **6** (an SiTBC).

Table 1. Elution velocity of three SiPc derivatives (**3b**, **4b**, **5b**) and **6**.[a]

Compound	M_r	v [cm min^{-1}]
Si–Si dimer **3b**	1562.76	0.50
monomer **4b**	798.38	0.44
μ-oxo dimer **5b**	1578.75	0.51
SiTBC **6**	658.22	0.32

[a] Gel-permeation chromatography (Bio-beads S-X1) was carried out on a 3.5×100 cm column. The dimers and the monomer **4b** were separated by about 15 cm at the bottom.

(0.51 cm min^{-1}), but distinctly larger than that of the corresponding Si monomer **4b** (0.44 cm min^{-1}; on a 3.5×100 cm column, dimer and monomer were separated by about 15 cm at the bottom) or **6** (0.32 cm min^{-1}). Since larger molecules are eluted faster in GPC and given the accuracy of recent GPC experiments,[10d] the data in Table 1 and Figure 5 indicate that our Si–Si dimer **3b** is only slightly smaller than the μ-oxo dimer **5b**, but much larger than monomers **4b** and **6**. When the fully purified Si–Si dimer **3b** was passed through the Bio-beads S-X1 column again or through a Bio-beads S-X2 column, only one dimeric Pc fraction was eluted, and no monomer fraction was obtained; this indicates that the fast-eluting fraction is not an aggregated dimeric Pc.

Mass spectra: Detection of the molecular ion peak of the Si_2Pc_2 dimers was not easy because of the weakness of the Si–Si bond. We used various methods, of which the ESI-TOF method gave ion peaks relatively easily for many compounds. Examples are shown in Figure 6. In the spectra of **1b** (Figure 6A and B), peaks around 2269.3 correspond to the desired structure with two axial OH ligands, while those around 2291.2 correspond to **1b** in which one OH group is converted to ONa. The peaks around 1133.6 and 1156.6 correspond to octabutoxy SiPc with one axial OH or ONa group, respectively. The second example is shown for **3b** in Figure 6C and D. Clusters of peaks around 1563.6 and 781.3 correspond to the desired *tert*-butylated Si–Si Pc dimer with two axial OH ligands and *tert*-butylated SiPc monomer with one OH ligand. Figure 6E shows the isotopic cluster for compound **1c**, which has no peripheral substituents; it is completely superimposable on the calculated distribution for $[M+H]^+$ (Figure 6E′; in this figure, cluster peaks around 1143.1 correspond to **1c** with two axial OMe ligands, since $CHCl_3$/MeOH (1/1) was used as solvent for MS analysis). This

0947-6539/02/0806-1476 $ 17.50+.50/0 *Chem. Eur. J.* **2002**, *8*, No. 6

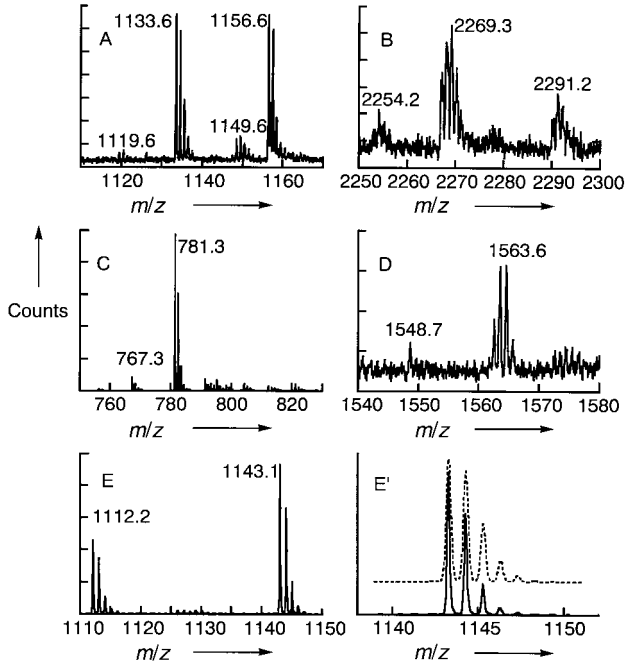

Figure 6. ESI-TOF mass spectra of Si–Si dimer **1b** (A, B), **3b** (C, D), and **1c** (E, E′). E′ is the parent-ion region of E, and the dotted line is the theoretical spectrum (solvent: methanol (**1b** and **3b**); chloroform/methanol = 1:1 (**1c**)).

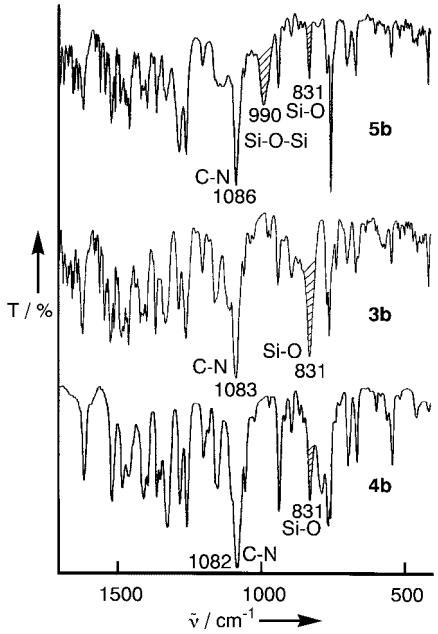

Figure 7. IR spectra of Si–Si dimer **3b**, SiPc monomer **4b**, and μ-oxo dimer **5b** (KBr pellet).

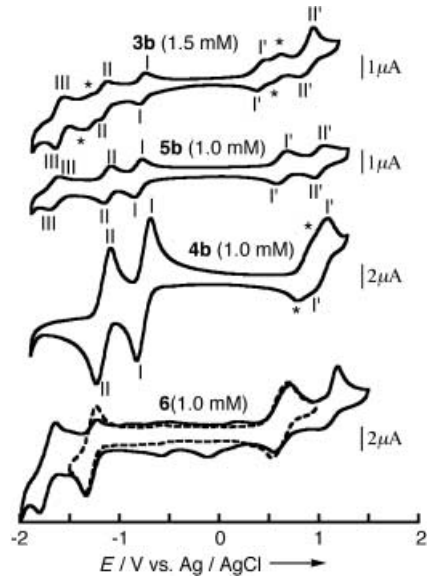

Figure 8. Cyclic voltamograms of Si–Si dimer **3b**, SiPc monomer **4b**, μ-oxo dimer **5b**, and SiTBC **6** in DCB with 0.1M TBAP. Sweep rate was 20 mV s^{-1}.

perfect correspondence precludes the other possibilities for its structure. The second set of peaks (ca. 50% intensity relative to the 1143 peak (100%)) corresponds to the structure with two axial OH ligands. Thus, as shown for the above three compounds, there is no indication of the presence of the SiTBC structure; the Pc macrocycle was always detected.

IR spectra: Si–Si bonds are readily cleaved and converted to Si-O-Si.[6] Therefore, evidence for the existence of an Si–Si bond in the dimer is of importance for assigning the structure. Figure 7 shows IR spectra of SiPcs with two OH groups as axial ligands in the region of 400–1700 cm^{-1}; that is the Si–Si dimer (*t*BuPcSiOH)$_2$ **3b**, Si monomer *t*BuPcSi(OH)$_2$ **4b**, and μ-oxo dimer (*t*BuSiPcOH)$_2$O **5b**. For all three compounds, the broad bands at around 3500 cm^{-1} were assigned to the O–H stretching vibration, and two sharp bands at about 831 and 1082–1086 cm^{-1} were assigned to the Si–O antisymmetric stretching vibration and C–N stretching vibration, respectively.[11] For the μ-oxo compound **5b**, a broad band at around 990 cm^{-1} was assigned to the Si-O-Si antisymmetric stretching vibration.[11] However, since the Si-O-Si band is absent for **3b**, its Si–Si bond may be retained in the structure. The similarity of the spectra reflects the common *t*BuPcSiOH partial structure of these three compounds.

Cyclic and differential pulse voltammetry: Figure 8 shows the cyclic voltammograms of **3b**, **4b**, **5b**, and **6**, and half-wave potentials $E_{1/2}$ and diffusion coefficient D are summarized in Table 2. Except for the aggregation couples (asterisks; currents in these couples increased with increasing concentration and decreasing sweep rate), within this potential window, two reduction couples and one oxidation couple were observed for the monomer **4b** ($E_{1/2} = -1.13$ (II), -0.73 (I),

Table 2. Redox potentials (vs. Ag/AgCl) and diffusion coefficients for Si–Si dimer **3b**, monomer **4b**, μ-oxo dimer **5b**, and SiTBC **6** in DCB containing 0.1M TBAP.

Compound	$E_{1/2}$ [V] 2nd oxid.	1st oxid.	1st redn.	2nd redn.	3rd redn.	D [cm^{2}s^{-1}]
4b		1.02	−0.73	−1.13		5.5×10^{-6}[a]
3b	1.02	0.50	−0.73	−1.13	−1.61	1.7×10^{-8}[a]
5b	0.99	0.61	−0.78	−1.10	−1.63	3.5×10^{-8}[b]
6	1.14	0.63	−1.22	−1.66		0.9×10^{-6}[c]

[a] Average calculated from the first and second reduction couples. [b] Average calculated from the first and third reduction couples. [c] Average calculated from the first oxidation and reduction couples.

and +1.02 V (I′)), while three reduction and two oxidation couples were observed for the μ-oxo dimer **5b** ($E_{1/2}$ = −1.63 (III), −1.10 (II), −0.78 (I), +0.61 (I′), and +0.99 V (II′)) and the Si–Si dimer **3b** ($E_{1/2}$ = −1.61 (III), −1.13 (II), −0.73 (I), +0.50 (I′), and 1.02 V (II′)). Except for the aggregation couples and oxidation couple II′ of **3b**, which were irreversible, the reversibility of other redox couples was indicated by a peak splitting of about 60 mV, a peak current ratio of 1.0, and constant $i_{p,c}/v^{1/2}$ values for potential sweep rates between 20 and 200 mV s^{-1}.[12] As shown by Kenney et al. for μ-oxo dimeric SiPcs, the redox couples of the μ-oxo dimer **5b** result from splitting of the redox couples in monomeric SiPcs, that is, in this case monomer **4b**.[13] The cyclic voltammogram of **3b** is similar in shape to that of the μ-oxo dimer **5b**, except for the regions of aggregation peaks, and this strongly suggests that compound **3b** is indeed a dimer (the number of redox couples of cofacial oligomers increases with increasing number of constituent units).[13] The voltammogram of **6** differs completely from those of the above three compounds in that the first reduction potential is much more negative, so that it is even more negative than the second reduction potentials of **3b**, **4b**, and **5b**. The first oxidation and reduction couples are reversible if the sweeps are returned after recording these couples between −1.5 and +1.0 V, while irreversibility increases if the potentials are widened to −2 to +1.5 V. In any case, there is no similarity between the voltammograms of the Si–Si Pc dimer **3b** and SiTBC **6**, and this precludes the possibility that **3b** contains the TBC structure.

Diffusion coefficients have been used as a measure of molecular size, generally becoming smaller with increasing molecular size. Accordingly, we determined values which from the cyclic voltammograms in Figure 8 for compounds **3b**, **4b**, **5b**, and **6**. The peak current in a cyclic voltammogram for a reversible system at room temperature is described by [Eq. (1)], where i_p [A] is the peak current, n the number of

$$i_p = 269 A n^{3/2} D^{1/2} C v^{1/2} \quad (1)$$

electrons, A [cm^2] the electrode area, D [cm^2 s^{-1}] the diffusion coefficient, C [mol L^{-1}] the bulk concentration, and v [V s^{-1}] the sweep rate.[14] Accordingly, the observed i_p depends on the value of D. As shown in Table 2, the D values for the monomer **4b** and **6** are on the order of 10^{-6} cm^2 s^{-1} (as the average for the first and second reduction couples, and for the first oxidation and reduction couples, respectively), which is similar to those of Pc and porphyrin monomers.[15] The values for the μ-oxo dimer **5b** and the Si–Si dimer **3b** were both on the order of 10^{-8} cm^2 s^{-1}, which is smaller than that of monomeric **4b** but reasonable, since these molecules are considered to be dimers. Thus, the results of cyclic voltammograms and diffusion coefficient data also support the conclusion that compound **3b** is a dimer.

Absorption and MCD spectroscopy and band deconvolution analysis: Figure 9 shows the electronic absorption and MCD spectra of **3b**, **4b**, and **5b**. The spectrum of monomer **4b** is typical for mononuclear Pcs, and shows Q_{00} and Soret bands at 681 and 357 nm, respectively.[16] Both the Q and Soret bands of the μ-oxo dimer **5b** are blue-shifted relative to those of the

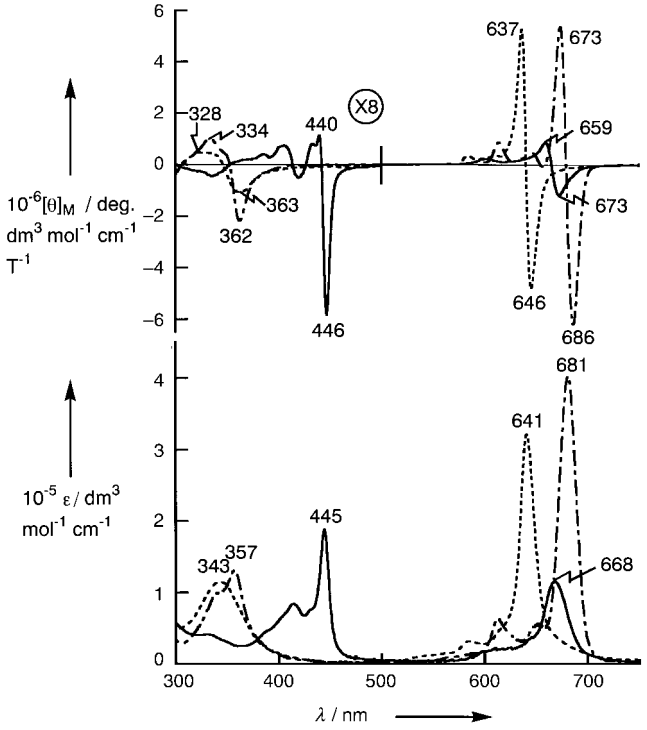

Figure 9. Absorption (bottom) and MCD (top) spectra of Si–Si dimer **3b** (——), SiPc monomer **4b** (•–•–), and μ-oxo dimer **5b** (- - - -) in $CHCl_3$.

monomer **4b**, and this kind of shift has been explained successfully in terms of exciton interaction.[17] The Q band of **3b** is also shifted to shorter wavelength, but only by about 15 nm (290 cm^{-1}), as opposed to 40 nm (920 cm^{-1}) in the μ-oxo dimer **5b**, and its absorption coefficient ε is much smaller than that of **5b**. Since exciton interaction becomes larger when two chromophores approach each other,[17] the smaller blue shift of the Q band in the Si–Si dimer **3b** compared to the μ-oxo dimer **5b** suggests that the electronic structures in these two compounds are different. This conjecture is strongly supported by comparison of the Soret band regions. The main band in this region shifts to the red to 445 nm from 357 nm for the monomer **4b** (by more than 90 nm (5540 cm^{-1})), with an associated large increase in intensity (area). Such a large red shift and band intensification on formation of the cofacial dimer can not be interpreted by exciton interaction, and this suggests that the band at 445 nm may have a different origin (these peculiar spectroscopic characteristics of the Si–Si dimer **3b** are clarified below, in the section on MO calculations).

In the MCD spectrum of **3b**, a dispersion curve (plausibly a Faraday A term, and less likely two interacting B terms[16a]), which was much lower in intensity (about 1/5) than that of **4b**, appeared at about 640 – 680 nm, which explicitly indicates that the two silicon atoms lie in the centers of the Pc skeletons. Otherwise, this dispersion-type curve would be more asymmetrical, and its inflection point would deviate considerably from the Q_{00} absorption peak position. To confirm the involvement of a Faraday A term, band deconvolution analysis was carried out over the Q-band region of compound **1b**, which does not contain isomers (Figure 10 and Supporting Information). Band deconvolution, which isolates the re-

0947-6539/02/0806-1478 $ 17.50+.50/0 *Chem. Eur. J.* **2002**, *8*, No. 6

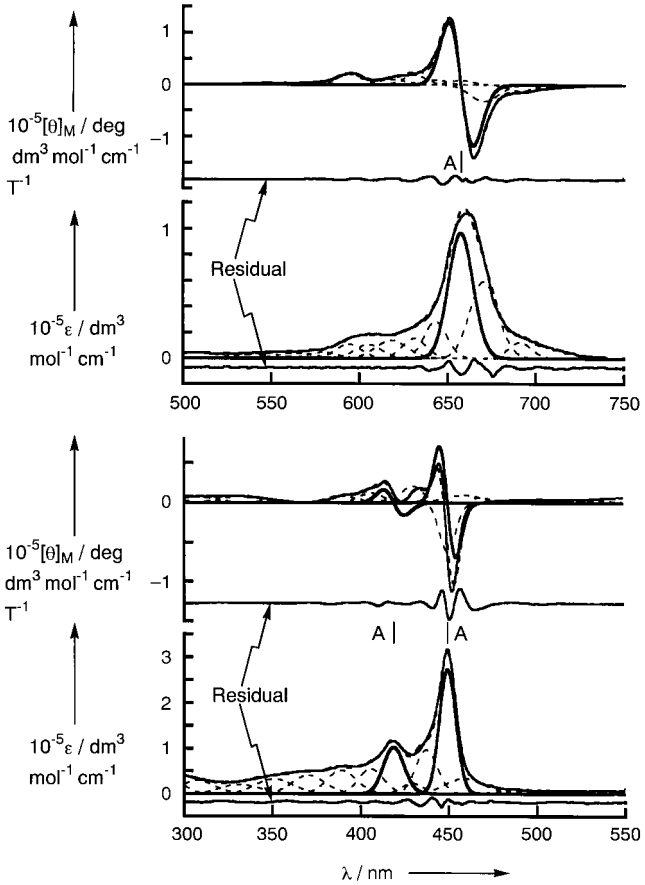

Figure 10. Deconvolution analysis of the Q- (top) and Soret-band (bottom) regions of Si–Si dimer **1b** (**3b** was not used for this purpose, since it is a mixture of isomers due to the positions of the *tert*-butyl groups). Solid lines: experimental data and residuals; Bold solid lines: individual bands; Dotted lines: fitted data.

quired bands from spectra by fitting each band with a Gaussian line shape, was rigorously developed by Stillman et al., and it is virtually the only way of accessing the transitions responsible for bands that overlap to any extent. As was reported previously,[18] linking the absorption and MCD spectra remarkably enhances the reliability of band deconvolution calculations. In other words, band centers and bandwidths were kept identical for the associated bands in both spectra, to reduce the ambiguity of the results. As seen in this figure, a dispersion-type MCD *A* term is indeed involved in the Q_{00} band region. In a cofacial dimer such as compound **3b**, the presence of an *A* term (i.e., the upper state degeneracy) is predicted if the molecular symmetry is either D_{4d} or D_{4h}. Thus, it seems clear that the Si–Si dimer **3b** contains silicon atoms at the centers. In the Soret band region, band deconvolution shows that the bands at 420 and 450 nm must contain MCD *A* term elements (band nos. 17 and 20 in the table in the Supporting Information) to fit the absorption and MCD spectra. This suggests that this region has transitions to degenerate excited states. The band elements at 437.4 (no. 18) and 406.0 nm (no. 21) can be assigned to the vibrational bands of *A* term elements. The other band elements at about 370–470 nm can be assigned to n–π* transitions involving oxygen lone pairs, since all alkoxy-substituted Pcs show this band.[19]

The blue shift and lowering of intensity of the Q band of **3b** compared with that of **4b** are expected on formation of a cofacial dimer.[17] However, the large red-shift of the main band in the Soret band region of **3b** is unique, since the Soret bands of most of the cofacial Pc dimers so far reported appeared at shorter wavelengths than those of monomers.[16a] Such a change cannot be predicted easily in a qualitative way, and so, to explain the change, MO calculations were attempted.

MO calculations

Equilibrium geometry of the Pc dimers and a model compound: Table 3 summarizes the optimized geometry (Figure 11) of the model compound $(TAPSiOH)_2$ and $(PcSiOH)_2$. Two possibilities are considered for each system. The first case is D_{4d} symmetry in which the two macrocycles are rotated by 45° around the Si–Si axis with respect to each other. The second is the case with D_{4h} symmetry in which the two macrocycles have an eclipsed conformation. The calculation for $(TAPSiOH)_2$ shows that the D_{4d} structure is more stable than the D_{4h} structure. Both the HF/6-31G and HF/3-21G energies for the D_{4d} structures are lower than corresponding energies of the D_{4h} structures. The energy difference

Table 3. Equilibrium geometries and energies calculated with HF/6-31G and HF/3-21G for the Pc dimer and TAP dimer (the results with 3-21G are in parentheses).

Molecule	D_{4d} $(TAPSiOH)_2$	D_{4h} $(TAPSiOH)_2$	D_{4d} $(PcSiOH)_2$	D_{4h} $(PcSiOH)_2$
HF energy[a]	−2819.9338	−2819.9163		
	(−2805.4678)	(−2805.4508)	(−4019.9745)	(−4019.9530)
r(Si–Si)[b]	2.576 (2.569)	2.708 (2.720)	(2.587)	(2.726)
r(Si–O)[b]	1.753 (1.687)	1.758 (1.702)	(1.686)	(1.690)
d(N1)[b]	1.442 (1.497)	1.526 (1.497)	(1.406)	(1.497)
d(C1)[b]	1.639 (1.657)	1.707 (1.657)	(1.558)	(1.652)
d(N2)[b]	1.696 (1.698)	1.759 (1.698)	(1.602)	(1.689)
d(C2)[b]	1.882 (1.866)	1.940 (1.866)	(1.738)	(1.859)

[a] In hartree. [b] In ångström.

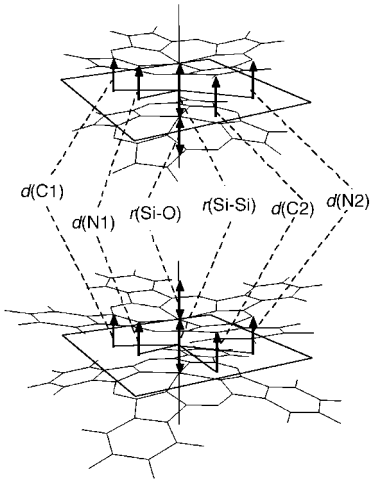

Figure 11. Tetraazaporphyrin (TAP) Si–Si dimeric structure used for calculations (Pc dimer was too large for a 6-31G set, so TAP, which corresponds to the core structure of Pc, was used).

is 0.0175 hartree (0.476 eV) at the HF/6-31G level, and 0.0170 hartree (0.462 eV) at HF/3-21G. In the HF/6-31G calculation the Si–Si bond length is predicted to be 2.576 Å, which is about 0.2 Å longer than the Si–Si single bond in hexachlorodisilane (2.34 ± 0.06 Å). This indicates that the Si–Si bond in the Pc dimer is essentially a single bond.

The HF/3-21G calculations on $(PcSiOH)_2$ indicate that the D_{4d} structure is again more stable. Although calculations with a larger basis would be desirable, the energy difference (0.0215 hartree, 0.585 eV) between the two structures decisively favours the D_{4d} structure. The calculated r(Si–Si), r(Si–O), d(N1), and d(C1) are very close to those of $(TAPSiOH)_2$. This indicates that as far as the central ring system is concerned, the structure is well described by the model. In the later section on XANES measurements, we therefore employ the $(TAPSiOH)_2$ structure for the analysis of the XANES peaks assigned to the Si atoms.

MO energy levels and characters: The left-hand side of Figure 12 shows the MO levels of monomeric $PcSi(OH)_2$. All the orbitals in this energy region are of π character. As is general for phthalocyanine compounds having no metal

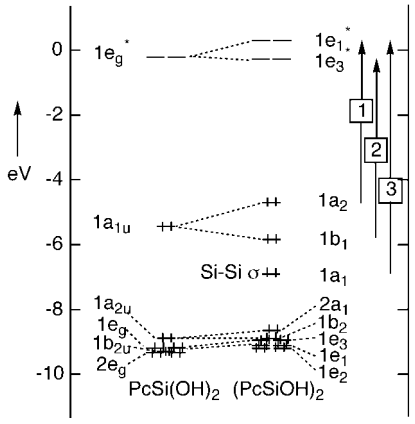

Figure 12. The energy levels of the HOMOs and LUMOs of D_{4h} $PcSi(OH)_2$ (left) and D_{4d} $(PcSiOH)_2$ (right). The former set was calculated with HF/6-31G at the optimum HF/6-31G equilibrium structure, and the latter with HF/3-21G at HF/3-21G equilibrium structure.

valence orbital in this region, $PcSi(OH)_2$ has a_{1u} HOMO, a_{2u} next HOMO, and e_g LUMO. The MOs of the dimeric D_{4d} $(PcSiOH)_2$ are shown in the right-hand side. Upon dimerization, each monomer MO is expected to interact with its counterpart to form dimer MOs, as was previously shown for dimeric lanthanide Pc compounds by Ishikawa et al.[20] From monomer a_{1u} HOMO, the a_2 and b_1 orbitals of the dimer are constructed, whereby the former are an antibonding combination and the latter a bonding combination. Similarly, the monomer a_{2u} next HOMO gives antibonding a_1 and bonding b_2 orbitals in the dimer. The e_g LUMO gives antibonding e_1 and bonding e_3 orbitals.

The most remarkable difference from the general "dimerization process" is the emergence of an additional MO between the MOs originating from the a_{1u} HOMO and the a_{2u} next-HOMO. The new MO ($1a_1$ in Figure 12) lies between the $1b_1$ and $2a_1$ orbitals. The shape of the MO (Figure 13, middle)

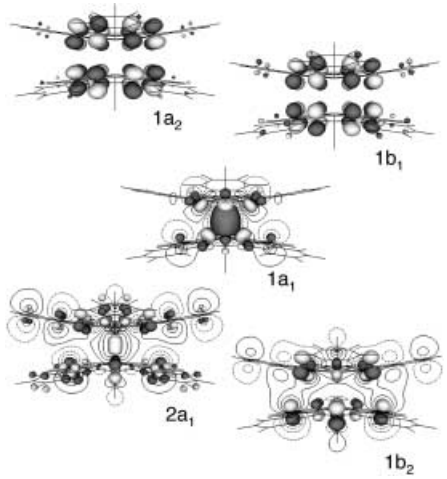

Figure 13. Isosurfaces and contour maps of the HOMOs of D_{4d} $(PcSiOH)_2$ calculated with HF/3-21G at the optimum HF/3-21G equilibrium structure. The contour maps show the values on a plane which contains the silicon atoms and *meso*-nitrogen atoms.

clearly shows that the orbital is essentially a σ bond between the two Si atoms.

The formation of the Si–Si σ bond can be viewed as follows. As a starting point, two Si^{III} ions, two OH^- ligands, and two Pc^{2-} ligands are chosen. Si sp hybrid orbitals are constructed from 3s and $3p_z$ orbitals for axial bonding. Vacant $3p_x$ and $3p_y$ orbitals accept lone pairs from coordinating nitrogen atoms of the Pc ligand to form Si–N bonds. The outward-pointing sp hybrid is vacant and accepts a lone pair from OH^- to form an Si–O bond. The inward-pointing sp hybrid contains one electron and forms a σ bond with the counterpart sp hybrid of the other Si atom. Since the counterpart antibonding Si–Si σ orbital is unoccupied, it is concluded that the Pc dimeric structure is formed by an Si–Si single bond. This Si–Si σ bond is the only valence bond which is not present in $PcSiOH_2$ monomer or in μ-oxo SiPc dimer.

Excited states and assignments of the absorption bands: Because of the presence of the new $1a_1$ MO just below the a_{1u}-origin HOMOs, a new electronic transition involving the MO is expected to be observed above the Q-band region. In fact, $1e_1^* \leftarrow 1a_1$ transition is symmetry allowed and can have a nonzero intensity.

Table 4 shows the results of the ab initio CIS calculation on the lowest four allowed E_1 excited states of $(PcSiOH)_2$. The first two E_1 states are basically $\pi-\pi^*$ transitions within Pc ligands. The $1E_1$ state is mainly composed of transition from the antibonding $1a_2$ HOMO to the antibonding $1e_1^*$ LUMO (arrow 1 in Figure 12). The main band in the Q band manifold observed at 668 nm (15.0×10^3 cm^{-1}) should be assigned to this state.

The main component of the $2E_1$ state is the excited transition from the bonding $1b_1$ HOMO to the bonding $1e_3^*$ LUMO (arrow 2 in Figure 12). A corresponding band is expected to be found in the Q-band manifold. However, such a band is not clearly identifiable in the observed spectrum. Nonetheless, since calculations at the CIS level generally contain errors of about 1 eV in the predicted excitation

0947-6539/02/0806-1480 $ 17.50+.50/0 *Chem. Eur. J.* **2002**, *8*, No. 6

Table 4. Calculated allowed singlet excited states of $(PcSiOH)_2$ and $PcSi(OH)_2$.

	State	Energy [10^3 cm^{-1}]	f	Configuration	Coefficient	Character[a]
$(PcSiOH)_2$	$1E_1$	18.5	0.70	$1a_2 \rightarrow 1e_1^*$	0.93	HOMO(ab) → LUMO(ab)
				$1b_1 \rightarrow 1e_3^*$	0.19	HOMO(b) → LUMO(b)
				$1a_1 \rightarrow 1e_1^*$	0.19	
	$2E_1$	22.2	0.41	$1b_1 \rightarrow 1e_3^*$	0.91	HOMO(b) → LUMO(b)
				$1a_1 \rightarrow 1e_1^*$	−0.25	HOMO(ab) → LUMO(ab)
				$1b_2 \rightarrow 1e_3^*$	−0.18	
	$3E_1$	27.6	0.33	$1a_1 \rightarrow 1e_1^*$	0.92	Si–Si σ → LUMO(ab)
				$1b_1 \rightarrow 1e_3^*$	0.24	
	$4E_1$	40.5	0.05	$1b_2 \rightarrow 1e_3^*(1)$	−0.53	
				$1e_2(1) \rightarrow 1e_3^*(1)$	−0.30	
				$1e_2(2) \rightarrow 1e_3^*(2)$	0.30	
$PcSi(OH)_2$	$1E_u$	18.8	0.85	$1a_{1u} \rightarrow 1e_g^*$	0.93	HOMO → LUMO
	$2E_u$	40.8	0.01	$1b_{2u} \rightarrow 1e_g^*$	0.67	
	$3E_u$	42.7	2.06	$1a_{2u} \rightarrow 1e_g^*$	0.68	
	$4E_u$	46.2	0.75	$1a_{2u} \rightarrow 1e_g^*$	0.55	
				$1a_{1u} \rightarrow 2e_g^*$	0.42	

[a] b = bonding, ab = antibonding character.

energies, we cannot exclude the possibility that $1E_1$ and $2E_1$ states are actually much closer, so that the two bands appear as a single band. In addition, the oscillator strength of the $2E_1$ state may have been overestimated, given the small size of the basis set employed. The positions and the relative intensities of the two bands in the Q-band region are an issue that should be examined in future.

The third allowed E_1 state is predominantly described by the transition from the Si–Si σ orbital to the antibonding $1e_1^*$ LUMO (arrow 3 in Figure 12). The calculation shows that the band has substantial oscillator strength and is well separated from the next $4E_1$ state, which is a π – π transition belonging to the B-band manifold. This indicates that the band at 445 nm between the Q-band and B-band regions should be assigned to the $3E_1$ state. From the character of the main configuration, the band can be referred to as "MMLCT" (metal – metal bond to ligand charge transfer) state. To our knowledge, this is the first clear observation of a band with such a character. In contrast, $PcSi(OH)_2$ does not have such an excited state associated with Si-centered orbital in the visible region (Table 4).

Resemblance of UV/Vis spectra of the Pc dimer and the TBC complex from the viewpoint of CIS calculations: Table 5 lists the result of the CIS calculation on TBCSiOH. The two lowest excited states, 1A′ and 1A″, have similar oscillator strengths. Although the predicted energy difference is relatively large, both states should be assigned to the band observed at about 680 nm for TBC complexes. An MCD measurement showed that the band has a pseudo-*A*-term spectral pattern, which supports the coincidental degeneracy of 1A′ and 1A″ states.[21] Comparison of Table 4 and Table 5 reveals that the energy of $1E_1$ in $(PcSiOH)_2$ and that of 1A″ in TBCSiOH are very close. Also, $2E_1$ in $(PcSiOH)_2$ and 1A′ in TBCSiOH are predicted to have similar energy. These similarities in the CIS calculations for the two cases are consistent with the coincidental resemblance of the UV/Vis spectra.

Table 5. CIS/6-31G allowed singlet excited states of TBCSiOH.

State	Energy [10^3 cm^{-1}]	f	Configuration	Coefficient	Character
1A″	19.7	0.43	1a″ → 1a′*	0.91	HOMO → LUMO(1)
			1a′ → 1a″*	−0.34	next HOMO → LUMO(2)
1A′	23.3	0.52	1a″ → 1a″*	0.91	HOMO → LUMO(2)
			1a′ → 1a′*	0.32	next HOMO → LUMO(1)
2A″	36.4	2.52	1a′ → 1a″*	0.87	next HOMO → LUMO(2)
			1a″ → 1a′*	0.32	HOMO → LUMO(1)
2A′	38.1	1.82	1a′ → 1a′*	0.89	next HOMO → LUMO(1)
			1a″ → 1a″*	0.33	HOMO → LUMO(2)

XANES spectra: X-ray absorption spectra are generally divided into two main regions.[22] First, XANES (X-ray absorption near edge structure), in the energy range of about 40 eV above the edge, provides information on stereochemistry (coordination geometry, bond angles, and relative positions of the neighboring atoms) that is particularly important for complex systems, characterized by weak order and low symmetry. Second, the higher energy extended X-ray absorption fine structure (EXAFS) region gives information on local structures in terms of atomic radial distribution (distances) around the central atom. Thus, this spectroscopic method appears to be appropriate for characterizing and differentiating SiPc monomer and Si–Si Pc dimers. Figure 14 shows the X-ray absorption spectra for SiPc monomer **4b** and Si–Si Pc dimer **3b**. In these spectra, EXAFS modulations were not sufficient to obtain an adequate result, so that EXAFS analysis was not carried out. In the XANES patterns of these spectra, some remarkable features were found. The dimer **3b** has a sharp peak at 1807 eV, while the monomer **4b** has a broader one around the same region. In the main peak at about 1810 eV, the monomer has one sharp peak, while the dimer has a broader peak, shifted to higher energy, which may include two or more subpeaks. In addition, the monomer has a small peak at 1813 eV, while in contrast, the dimer has two very small and wider peaks at about 1816 and 1822 eV. Transitions obtained from the DV calculations are also shown in this figure. Calculated transition energies were convoluted by using a Gaussian function with a full-width half-height (FWHH) of 1.0 eV. Energy scales are calibrated to a relative value, as the energy value of the Si *K*-edge is 0 eV. Orbitals shown under the transitions are the main molecular orbital components. Orbitals in italics originate from the atoms in the molecule on the opposite side. Calculated transitions and experimental XANES spectra are shown in the same figure. Each result shows a good fit between experiment and calculation, that is, the calculated results and conditions are appropriate. Analysis was performed by comparing the experimental and calculated spectra. As shown by the main components for molecular orbitals, the peak at 1807 eV in the

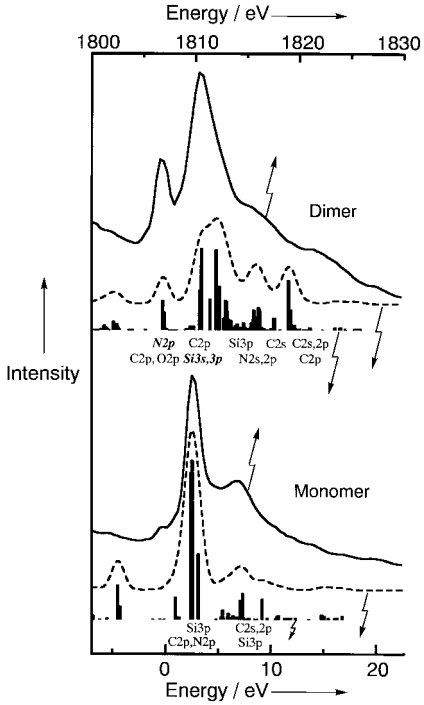

Figure 14. Si *K*-edge XANES spectra (solid lines) of Si–Si dimer **3b** (top) and SiPc monomer **4b** (bottom) and calculated XANES spectra (broken lines) of $(TAPSiOH)_2$ (top) and TAPSiOH (bottom). For calculated Si *K*-edge XANES spectra, the energy scale is normalized to the Si *K*-edge at 0 eV. Calculated transitions are shown by bars, and orbitals under these are the main MO components. Orbitals in italics are MOs originating from atoms in the molecule on the opposite side.

dimer depends on the contribution of N 2p orbitals of the opposite side, and so this peak is considered to be especially characteristic of the dimer. The peak at 1810 eV in the monomer is divided into two peaks at 1811 and 1813 eV in the dimer. This result also shows the contribution of the interactions from the Si 3s and 3p orbitals from the opposite side. In the spectrum of the monomer, the peaks ascribed to Si 3p orbitals are concentrated at about 1817 eV; however, the dimer has several small peaks spread over a wide range. This phenomenon may also be characteristic of dimerization. The dimer and monomer samples have thus characterized by XANES spectra and molecular model calculations, which reveal complex interactions that include not only an Si–Si bond but also a strong contribution of N atoms from the opposite side. This result shows that the structure of the ligand molecule has an important role in the dimerization.

Conclusion

The structures of Pcs synthesized by means of a one-pot, one-step condensation of 1*H*-isoindole-1,3(2*H*)-diimine in the presence of hexachlorodisilane were characterized by GPC, MS, NMR, IR, and CV. All data suggested that the products are cofacial Pcs with a direct Si–Si linkage which are slightly smaller than the μ-oxo dimer of the corresponding Pc. The characteristic UV/Vis and MCD spectra of the dimer were explained by MO calculations and band deconvolution techniques. In particular, a characteristic band observed for Si–Si Pc dimers was assigned to a charge-transfer transition from an Si–Si σ-bonding orbital to a ligand π* orbital. Furthermore, in the Si *K*-edge XANES spectrum of an Si–Si Pc dimer, some signals were detected which were not observed for the corresponding monomer. The XANES spectra of both the monomer and dimer were reproduced by quantum mechanical simulations, and the signals seen only for the dimer were reasonably interpreted as being produced by interactions between the atoms on the opposite side (Si or Pc plane). In this way, we have obtained and characterized directly linked Si–Si Pc dimers using the method reported previously.[2] Furthermore, we succeeded in obtaining single crystals of triethylsiloxy(tetrabenztriazacorrolato)silicon. This compound is indeed diffrerent from the above Si–Si Pc dimers in its size and electrochemical properties, but showed an electronic spectrum similar to those of the Si–Si Pc dimers, which was also interpreted by MO calculations.

Experimental Section

Measurements: GPC for purification of the compounds and estimation of molecular size was carried out on a Bio-beads S-X1 (Bio-rad) column (3.5×100 cm) with chloroform or THF as eluent. Mass spectra were measured on a Perseptive Biosystem MALDI-TOF Mass Voyager DE-SI2 spectrometer with dithranol (1,8,9-anthracenetriol) as matrix, on a Micromass LCT-ESI-TOF mass spectrometer with methanol or chloroform/methanol as solvent, and on a JEOL SX-102 mass spectrometer (FAB mass) with *p*-nitrophenyl *n*-octyl ether or *m*-nitrobenzyl alcohol (NBA) as matrix. Field desorption (FD) mass spectra were recorded on a VG Zabspec spectrometer with NBA as matrix. Electronic (UV/Vis) and FT-IR spectra were recorded on Hitachi U-3410 and Shimazu FTIR-8100M spectrometers, respectively. MCD measurements were made with a JASCO J-725 spectrodichrometer equipped with a Jasco electromagnet that produced magnetic fields of up to 1.09 T with parallel and then antiparallel field. Its magnitude was expressed in terms of molar ellipticity per tesla, $[\theta]_M/10^5$ deg mol^{-1} dm^3 cm^{-1} T^{-1}. The 400 MHz ^{1}H NMR spectra were recorded with a JEOL GSX-400 spectrometer in C_6D_6 and $CDCl_3$. CV was performed with a Hokuto Denko HA-501 potentiostat/galvanostat connected to a Hokuto Denko HB-105 function generator and a Graphtec WX 1200 recorder. A glassy carbon electrode (area 7 mm^2) was used as the working electrode, a platinum wire as the auxiliary electrode, and Ag/AgCl as the reference electrode. Tetrabutylammonium perchlorate (TBAP), recrystallized from absolute ethanol, was used as the supporting electrolyte (0.1M solution). All electrochemical experiments were carried out in *o*-dichlorobenzene (DCB) at 298 ± 0.5 K under a dry nitrogen atmosphere. The XANES spectra were recorded on powder samples. Si *K*-edge spectra (1.8 keV) were collected at the UVSOR of Institute for Molecular Science in Japan, at room temperature and under high vacuum. Monochromatic radiation was obtained by using an InSb(111) ($d = 3.740$ Å) monochromator.

X-ray crystal structure analysis was performed on a Rigaku/MSC Mercury CCD diffractometer with graphite-monochromated $Mo_{K\alpha}$ radiation ($\lambda =$ 0.71070 Å). All calculations were performed with the teXsan crystallographic software package[23] on a Silicon Graphics O_2 computer.

Bis[hydroxy(2,3,9,10,16,17,23,24-octabutoxyphthalocyaninato)silicon] (1b): A mixture of 5,6-dibutoxy-1*H*-isoindole-1,3(2*H*)-diimine[24] (580 mg, 2 mmol) and hexachlorodisilane (0.5 mL, 1.25 mmol) in fresh quinoline (3 mL) was heated at 180–190 °C for 20 min under nitrogen.[7] After cooling to room temperature, methanol/water was added to the reaction mixture, which was filtered, and the residue was washed with methanol and acetone. After recrystallization from chloroform/methanol, a dark green mixture (**1a** + **1b** + monomers, see Figure 2) was obtained. This mixture was dissolved in dichloromethane (30 mL) containing anion-exchange resin (Amberlyst A26) and refluxed for 2 h to convert the axial ligands completely from chloro to hydroxy.[25] After cooling to room temperature, the ion-exchange resin was removed by filtration, and the solvent

  0947-6539/02/0806-1482 $ 17.50+.50/0 *Chem. Eur. J.* **2002**, *8*, No. 6

evaporated under reduced pressure. The residue was purified by column chromatography on aluminum oxide (neutral, activity III) with chloroform as eluent, then recrystallized from chloroform/methanol to give 0.25 g of **1b** + monomers. The residue was then further separated by GPC on Bio-beads S-X1(Biorad) with chloroform, and recrystallized from chloroform/methanol to give the dimer **1b** (171 mg, 30.1 %) and monomers (65 mg, 10.7 %). ^{1}H NMR (400 MHz, [D$_6$]benzene): $\delta = 9.5-7.5$ (br, ArH, one peak at 8.44), 4.9–3.0 (br, OCH_2), 2.5–0 (br, $CH_2CH_2CH_3$), −1.8 to −2.0 (br, OH). MS (ESI-TOF, methanol): *m/z*: 2269.3 [*M*+H]; elemental analysis calcd (%) for $C_{128}H_{162}N_{16}O_{18}Si_2$ (2269.0): C 67.76, H 7.20, N 9.88; found: C 66.8, H 7.84, N 8.69.

Bis[hydroxy(phthalocyaninato)silicon] (1c): Compound **1c** was synthesized as for **1b** by using 1*H*-isoindole-1,3(2*H*)-diimine in place of 5,6-dibutoxy-1*H*-isoindole-1,3(2*H*)-diimine. MS (ESI-TOF, chloroform/methanol 1/1): *m/z*: 1143.1 [*M* − 2OH+2OMe], 1112.2 [*M* − 2H]; because of the low solubility, NMR spectra were not recorded.

Dimethoxy(2,3,9,10,16,17,23,24-octabutoxyphthalocyaninato)silicon (2c): A mixture of 5,6-dibutoxy-1*H*-isoindole-1,3(2*H*)-diimine[24] (61 mg, 0.212 mmol) and tetrachlorosilane (0.1 mL, 0.88 mmol) in fresh quinoline (2 mL) was heated at 180–190 °C for 1 h under nitrogen.[7] After cooling to room temperature, methanol/water was added to the reaction solution, and the solid was collected by filtration and washed with methanol and acetone. The residue was dissolved in dichloromethane (5 mL) containing ion-exchange resin to convert the axial ligands from chloro to hydroxy.[25] The monomer **2b** was obtained by purifying the green residue by column chromatography on aluminum oxide (neutral, activity III) with chloroform. A mixture of **2b** (0.88 mmol, assuming 100 % yield), NaH (70 mg, 1.8 mmol), and dimethyl sulfate (0.17 mL, 1.8 mmol) in dry THF (8 mL) was stirred at room temperature for two days. After the solvent had been evaporated, the dark green solid was purified by column chromatography on aluminum oxide (neutral, activity III) with chloroform, and recrystallized from chloroform/methanol to give the monomer **2c** (6.3 mg, 10 %). ^{1}H NMR (400 MHz, $CDCl_3$, 25 °C): $\delta = 8.996$ (s, 8H; ArH), 4.75–4.38 (br, 16H; OCH_2, one peak at 4.677), 2.171 (br, 16H; OCH_2CH_2), 1.790 (br, 16H; $O(CH_2)_2CH_2$), 1.213 (br, 24H; CH_3), −1.819 (s, 6H; OCH_3); MS (FAB, NBA): *m/z*: 1178 [*M*]; elemental analysis calcd (%) for $C_{66}H_{86}N_8O_{10}$-Si (1179.5): C 67.21, H 7.35, N 9.50: found: C 68.83, H 7.18, N 9.35.

Bis[hydroxy{2,9(or 10),16(or 17),23(or 24)-tetra-*tert*-butylphthalocyaninato}silicon] (3b): Similarly to **1b**, **3b** was prepared from 5-*tert*-butyl-1*H*-isoindole-1,3-(2*H*)-diimine (100 mg, 0.5 mmol) and hexachlorodisilane (0.1 mL) in quinoline at 180–190 °C for 20 min under nitrogen. Chromatography on aluminum oxide (neutral, activity III) and Bio-beads S-X1 with chloroform produced the desired compound **3b** (25 mg, 26 %). MS (ESI-TOF, methanol): *m/z*: 1563.6 [*M*]; elemental analysis calcd (%) for $C_{96}H_{98}N_{16}O_2Si_2$ (1564.1): C 73.72, H 6.32, N 14.33; found: C 72.94, H 6.76, N 15.01.

Dihydroxy{2,9(or 10),16(or 17),23(or 24)-tetra-*tert*-butylphthalocyaninato}silicon (4b): Compound **4b** was obtained by the method used for **2b** from 5-*tert*-butyl-1*H*-isoindole-1,3(2*H*)-diimine and $SiCl_4$. MS (MALDI-TOF, dithranol): *m/z*: 798 [*M*]; IR (KBr): $\tilde{\nu} = 831$ (SiO), 3450 cm^{-1} (OH); UV/Vis ($CHCl_3$): $\lambda_{max} = 681.5$ nm.

***μ*-Oxo-bis[hydroxy{2,9(or 10),16(or 17),23(or 24)-tetra-*tert*-butylphthalocyaninato}silicon] (5b)**: A dry solution of monomer **4b** (100 mg) in quinoline (3 mL) was refluxed for 80 min under nitrogen.[26] After the mixture had been cooled to room temperature, methanol and water were added to the reaction solution, and the resulting precipitate separated from the solution by filtration and dried under vacuum. This residue was purified by chromatography on aluminum oxide (neutral, activity III) and Bio-beads S-X1 with chloroform, to give pure **5b** as a blue powder (35 mg, 17.6 % yield). MS (MALDI-TOF, dithranol): *m/z*: 1578 [*M*]; IR (KBr): $\tilde{\nu} =$ 831 (SiO), 990 (SiOSi), 3450 cm^{-1} (OH); UV/Vis ($CHCl_3$): $\lambda_{max} = 641$ nm.

Triethylsiloxy(tetrabenztriazacorrolato)silicon (6): In the synthesis of compound **1c**, methanol was added to the reaction vessel after the reaction was complete, and the resultant precipitate of **1c** was collected by filtration. Then the solvent was evaporated from the filtrate, and the green residue (ca. 200 mg) was treated with triethylsilyl chloride (1 mL) at 50 °C for 3 h in dry pyridine (10 mL). After the mixture had been cooled to room temperature, the pyridine was removed by filtration, and the green residue applied to a basic alumina column (activity V) and eluted with toluene/pyridine (10/1) as eluent. The first-eluting blue band was not collected, while the second, green band was collected and recrystallized from CH_2Cl_2/MeOH to give 60 mg (24.7 %) of the desired compound as a green powder. Single crystals for X-ray analysis were grown from benzene. ^{1}H NMR (400 MHz, [D$_6$]benzene, 25 °C): $\delta = 9.83-9.78$ (m, 4H), 9.55–9.53 (m, 2H), 8.84–8.82 (m, 2H), 8.02–7.95 (m, 4H), 7.80–7.73 (m, 4H), −1.24 (t, 9H; CH_3), −2.18 (q, 6H; CH_2); MS (FAB, NBA): *m/z*: 659 [*M*+H]; IR (KBr): $\tilde{\nu} = 1003$ (SiOSi), 822 cm^{-1} (SiO); elemental analysis calcd (%) for $C_{38}H_{32}N_7O_1Si_2$ (658.89): C 69.27, H 4.90, N 14.88; found: C 68.85, H 4.62, N 14.91.

Methods of calculation

Optimization of ground-state geometry: Ab initio Hartree–Fock (HF) calculations were carried out to examine the equilibrium structure of the Pc dimer. Because the molecule is rather large for the ab initio method, we used a model molecule and applied several constraints to the structure. First, tetraazaporphyrin (TAP) was employed as a model for Pc (Figure 11). TAP has a Pc structure from which four benzenoid moieties have been removed, while retaining the same central ring structure as Pc. Second, the molecular structures were assumed to have D_{4d} or D_{4h} symmetry, whereby the Si-O-H angle was fixed at 180° to maintain the C_4 symmetry axis. The computational complexity is thus reduced by a factor of roughly 16, that is, is the number of the symmetry operations. The 3-21G and the superior but computationally more demanding 6-31G basis sets were used for the model $(TAPSiOH)_2$, but only 3-21G for $(PcSiOH)_2$. For the study on the TBC complex and monomeric Pc complex, model molecules with axial hydroxy ligands, namely, TBCSiOH and $PcSi(OH)_2$, were employed. The 6-31G basis set was used for the optimization of their structures. The structures of TBCSiOH and $PcSi(OH)_2$ were assumed to have C_s and D_{4h} symmetry, respectively.

The optimization calculations were performed with the Q-Chem quantum chemistry program package.[27]

Excited states: Excitation energies and oscillator strengths of allowed excited states of $(PcSiOH)_2$, TBCSiOH, and $PcSi(OH)_2$ were calculated by ab initio CIS (single excitation configuration interaction) method. The basis sets employed were 3-21G for $(PcSiOH)_2$ and 6-31G for TBCSiOH and $PcSi(OH)_2$. All the singly excited configurations were included in the calculations. The aforementioned HF structures were employed for the CIS calculations. For $(PcSiOH)_2$, the lowest four allowed excited states were calculated because of the large size of the molecule, which is computationally demanding. The excited-state calculations were carried out with Q-Chem.[27]

XANES fitting: The XANES spectra were analyzed by DV-X*α* MO calculations. The computational details of the DV-X*α* method have been previously described.[28] Each model for the monomer and dimer was built and refined using (TAPSiOH) and $(TAPSiOH)_2$ models. The atomic orbitals used for calculations were 1s for H, 1s–3p for C and O, and 1s–4p for Si. Sample points for the integration were set to 85 000. The transition states of (TAPSiOH) and $(TAPSiOH)_2$ were calculated to ascribe the XANES spectra.

X-ray structure analysis of SiTBC: CCDC 169864 contains the supplementary crystallographic data for this paper. These data can be obtained free of charge via www.ccdc.cam.ac.uk/conts/retrieving.html (or from the Cambridge Crystallographic Data Centre, 12 Union Road, Cambridge CB2 1EZ, UK; fax: (+44) 1223-336-033; or deposit@ccdc.cam.uk).

Acknowledgement

We thank Dr. Ayse G. Gurek for FD mass measurements. This research was supported partially by a Grant-in-Aid for Scientific Research (B) No. 11440192 and the Scandinavia-Japan Sasakawa Foundation.

[1] S. Nakamura, A. Flamini, V. Fares, M. Adachi, *J. Phys. Chem.* **1992**, *96*, 8351.
[2] Preliminary results: N. Kobayashi, F. Furuya, G.-C. Yug, *J. Porphyrins Phthalocyanines* **1999**, *3*, 433.
[3] M. Fujiki, H. Tabei, K. Isa, *J. Am. Chem. Soc.* **1986**, *108*, 1532.
[4] J. Li, L. R. Subramanian, M. Hanack, *Chem. Commun.* **1997**, 679.
[5] SiPcs with Cl atoms as axial ligands are stable only under dry-box conditions; their Cl atoms are gradually replaced by OH ions under

normal experimental conditions. Accordingly, they are often regarded as intermediates and are not well characterized. For example, see a) J. Kleinwachter, M. Hanack, *J. Am. Chem. Soc.* **1997**, *119*, 10684; b) J. F. Pol, J. W. Zwikker, J. M. Warman, M. P. Haas, *Recl. Trav. Chim. Pays-Bas* **1990**, *109*, 208.

[6] a) K. Naumann, G. Zon, K. Mislow, *J. Am. Chem. Soc.* **1969**, *91*, 7012; b) G. Zon, K. E. DeBruin, K. Naumann, K. Mislow, *J. Am. Chem. Soc.* **1969**, *91*, 7023.

[7] M. K. Lowery, A. J. Starshak, J. N. Esposito, P. C. Krueger, M. E. Kenney, *Inorg. Chem.* **1965**, *4*, 128.

[8] N. Kobayashi, A. B. P. Lever, *J. Am. Chem. Soc*. **1987**, *109*, 7433.

[9] Crystal data for TBCSiOSiEt$_3$: $C_{38}H_{31}ON_7Si_2$. $M_r = 657.88$, monoclinic, space group $P2_1/n$ (no. 14), $a = 8.9139(5)$, $b = 24.062(3)$, $c = 14.934(2)$ Å, $V = 3127.2(6)$ Å^3, $Z = 4$, $\rho_{calcd} = 1.397$ g cm^{-3}, $\mu(Mo_{K\alpha}) = 1.59$ cm^{-1}, $T = -30\,^{\circ}C$, crystal size $0.07 \times 0.15 \times 0.20$ mm, Rigaku/MSC Mercury CCD. Of a total of 16755 measured reflections, 6603 were independent; $R = 0.054$, $Rw = 0.062$ for 2790 observed reflections $[I > 3\sigma(I)]$, GOF 1.29, $\rho_{max./min.} = 0.22/-0.25$ e Å^{-3}. For more details, see Supporting Information.

[10] a) D. Lelièvre, L. Bosio, J. Simon, J. J. André, F. Bensebaa, *J. Am. Chem. Soc.* **1992**, *114*, 4475; b) G. C. Bryant, M. J. Cook, T. G. Ryan, A. J. Thorne, *J. Chem. Soc. Chem. Commun.* **1995**, 467; c) C. Sirlin, L. Bosio, J. Simon, *J. Chem. Soc. Chem. Commun.* **1988**, 236; d) R. A. Haycock, C. A. Hunter, D. A. James, U. Michelson, L. R. Sutton, *Org. Lett.* **2000**, *2*, 2435.

[11] a) B. L. Wheeler, G. Nagasubramanian, A. J. Bard, L. A. Schechtman, D. R. Dininny, M. E. Kenney, *J. Am. Chem. Soc.* **1984**, *106*, 7404; b) C. W. Dirk, T. Inabe, K. F. Schoch, Jr., T. J. Marks, *J. Am. Chem. Soc.* **1983**, *105*, 1539.

[12] a) H. Matsuda, Y. Ayabe, *Z. Elektrochem.* **1955**, *59*, 494; b) H. Matsuda, *Z. Elektrochem.* **1957**, *61*, 489.

[13] D. W. DeWulf, J. K. Leland, B. L. Wheeler, A. J. Bard, D. A. Batzel, D. R. Dininny, M. E. Kenney, *Inorg. Chem.* **1987**, *26*, 266.

[14] *Experimental Electrochemistry for Chemists* (Eds.: D. T. Sawyer, J. L. Robert, Jr.), Wiley-Interscience, New York, **1979**, p. 329.

[15] a) N. Kobayashi, Y. Nishiyama, *J. Phys. Chem.* **1985**, *89*, 1167; b) P. A. Forshey, T. Kuwana, N. Kobayashi, T. Osa in *Electrochemical and Spectrochemical Studies of Biological Redox Components*, *Advances in Chemistry Series 201* (Ed.: K. M. Kadish), ACS Publications, Washington, **1982**, p. 601.

[16] a) M. J. Stillman, T. Nyokong in *Phthalocyanines—Properties and Applications*, *Vol. 1* (Eds.: C. C. Leznoff, A. B. P. Lever), VCH, New York, **1989**, Chap. 3; b) N. Kobayashi, H. Konami in *Phthalocyanines—Properties and Applications*, *Vol. 4* (Eds.: C. C. Leznoff, A. B. P. Lever), VCH, New York, **1996**, Chap. 9; c) E. A. Luk′yanets, *Electronic Spectra of Phthalocyanines and Related Compounds*, NIOPIK, Moscow, **1989**.

[17] a) M. Kasha, H. R. Rawls, M. A. El-Bayoumi, *Pure Appl. Chem*. **1965**, *11*, 371; b) M. Gouterman, D. Holten, E. Lieberman, *Chem. Phys.* **1977**, *25*, 139.

[18] a) T. Nyokong, Z. Gasyna, M. J. Stillman, *Inorg. Chem.* **1987**, *26*, 1087; b) W. R. Browett, Z. Gasyna, M. J. Stillman, *J. Am. Chem. Soc.* **1988**, *110*, 3633; c) E. A. Ough, T. Nyokong, K. A. M. Creber, M. J. Stillman, *Inorg. Chem.* **1988**, *27*, 2724; d) Z. Gasyna, N. Kobayashi, M. J. Stillman, *J. Chem. Soc. Dalton Trans.* **1989**, 2397; e) Z. Gasyna, M. J. Stillman, *Inorg. Chem.* **1990**, *29*, 5101; f) E. A. Ough, Z. Gasyna, M. J. Stillman, *Inorg. Chem.* **1991**, *30*, 2301; g) J. Mack, M. J. Stillman, *Inorg. Chem.* **1992**, *31*, 1717; h) E. A. Ough, M. J. Stillman, *Inorg. Chem*. **1994**, *33*, 573; i) J. Mack, M. J. Stillman, *J. Am. Chem. Soc*. **1994**, *116*, 1292; j) J. Mack, M. J. Stillman, *J. Phys. Chem.* **1995**, *99*, 7935; k) J. Mack, M. J. Stillman, *Inorg. Chem*. **1997**, *36*, 413; l) J. Mack, N. Kobayashi, C. C. Leznoff, M. J. Stillman, *Inorg. Chem.* **1997**, *36*, 5624; m) E. A. Ough, K. A. M. Creber, M. J. Stillman, *Inorg. Chim. Acta* **1996**, *246*, 361.

[19] L. Guo, D. E. Ellis, B. M. Hoffman, Y. Ishikawa, *Inorg. Chem.* **1996**, *35*, 5304.

[20] N. Ishikawa, O. Ohno, Y. Kaizu, H. Kobayashi, *J. Phys. Chem.* **1992**, *96*, 8832.

[21] F. Furuya, N. Kobayashi, unpublished data.

[22] a) T. A. Smith, J. E. Penner-Hahn, M. A. Berding, S. Doniach, K. O. Hodgson, *J. Am. Chem. Soc.* **1985**, *107*, 5945; b) A. Bianconi, A. Giovannelli, L. Castellani, *J. Mol. Biol.* **1983**, *165*, 125.

[23] teXan: Crystal Structure Analysis Package, Molecular Structure Corporation, **1985**, **1999**.

[24] D. Wöhrle, V. Schmidt, *J. Chem. Soc. Dalton Trans.* **1988**, 549.

[25] T. Sauer, G. Wegner, *Mol. Cryst. Liq. Cryst.* **1988**, *162B*, 97.

[26] E. Ciliberto, K. A. Doris, W. J. Pietro, G. M. Reisner, D. E. Ellis, I. Fragalà, F. H. Herbstein, M. A. Ratner, T. J. Marks, *J. Am. Chem. Soc.* **1984**, *106*, 7748.

[27] C. A. White, J. Kong, D. R. Maurice, T. R. Adams, J. Baker, M. Challacombe, E. Schwegler, J. P. Dombroski, C. Ochsenfeld, M. Oumi, T. R. Furlani, J. Florian, R. D. Adamson, N. Nair, A. M. Lee, N. Ishikawa, R. L. Graham, A. Warshel, B. G. Johnson, P. M. W. Gill and M. Head-Gordon, Q-Chem, Version 1.2, Q-Chem, Inc., Pittsburgh, PA, **1998**.

[28] a) H. Adachi, M. Tsukada, C. Satoko, *J. Phys. Soc. Jpn.* **1978**, *45*, 875; b) C. Satoko, M. Tsukada, H. Adachi, *J. Phys. Soc. Jpn.* **1978**, *45*, 1333; c) H. Adachi, S. Shiokawa, M. Tsukada, C. Satoko, *J. Phys. Soc. Jpn.* **1979**, *47*, 1528.

Received: January 2, 2001
Revised: November 8, 2001 [F2981]

  0947-6539/02/0806-1484 $ 17.50+.50/0